Dynamic causal modeling of cortical activity from the acute to the chronic stage after stroke

Anne K. Rehme[a], **Simon B. Eickhoff**[b,c], **Ling E. Wang**[a,c], **Gereon R. Fink**[c,d], **Christian Grefkes**[a,d,*]

[a]Neuromodulation & Neurorehabilitation, Max Planck Institute for Neurological Research Cologne, Germany

[b]Department of Psychiatry and Psychotherapy, RWTH Aachen University, Germany

[c]Institute of Neurosciences and Medicine (INM-2, INM-3), Jülich Research Centre, Germany

[d]Department of Neurology, University of Cologne, Germany

Abstract

Functional neuroimaging studies frequently demonstrated that stroke patients show bilateral activity in motor and premotor areas during movements of the paretic hand in contrast to a more lateralized activation observed in healthy subjects. Moreover, a few studies modeling functional or effective connectivity reported performance-related changes in the motor network after stroke. Here, we investigated the temporal evolution of intra- and interhemispheric (dys-) connectivity during motor recovery from the acute to the early chronic phase post-stroke. Twelve patients performed hand movements in an fMRI task in the *acute* (72 hours) and *subacute stage* (2 weeks) post-stroke. A subgroup of 10 patients participated in a third assessment in the *early chronic stage* (3–6 months). Twelve healthy subjects served as reference for brain connectivity. Changes in effective connectivity within a bilateral network comprising M1, premotor cortex (PMC), and supplementary motor area (SMA) were estimated by dynamic causal modeling. Motor performance was assessed by the Action Research Arm Test and maximum grip force. Results showed reduced positive coupling of ipsilesional SMA and PMC with ipsilesional M1 in the acute stage. Coupling parameters among these areas increased with recovery and predicted a better outcome. Likewise, negative influences from ipsilesional areas to contralesional M1 were attenuated in the acute stage. In the subacute stage, contralesional M1 exerted a positive influence on ipsilesional M1. Negative influences from ipsilesional areas on contralesional M1 subsequently normalized, but patients with poorer outcome in the chronic stage now showed enhanced negative coupling from contralesional upon ipsilesional M1. These findings show that the reinstatement of effective connectivity in the ipsilesional hemisphere is an important feature of motor recovery after stroke. The shift of an early, supportive role of contralesional M1 into enhanced inhibitory coupling might indicate maladaptive processes which could be a target of non-invasive brain stimulation techniques.

---

[*]Corresponding author. Max Planck Institute for Neurological Research, Gleueler Str. 50, 50931 Cologne, Germany. Christian.Grefkes@uk-koeln.de (C. Grefkes).

Keywords

Motor cortex; Longitudinal; Effective connectivity; Impairment; Recovery

Introduction

Functional neuroimaging studies investigating stroke patients with motor deficits frequently reported that unilateral movements of the paretic limb are associated with a more bilateral activation pattern in primary motor and premotor areas as compared to neural activity assessed during unilateral hand movements in healthy subjects (Chollet et al., 1991; Grefkes et al., 2008b; Ward et al., 2003; Weiller et al., 1992). However, the neural processes underlying functional activity and their implication for motor recovery are still controversial (Bütefisch et al., 2005; Fridman et al., 2004; Gerloff et al., 2006; Johansen-Berg et al., 2002; Ward et al., 2003). Recent advances in modeling neural responses allow estimating effective connectivity within neural networks from functional neuroimaging time series (Friston et al., 2003; Stephan et al., 2007, 2010). Effective connectivity is defined as the influence that one brain region exerts over another (Friston et al., 2003). Hence, changes in effective connectivity in a functional network after stroke might constitute one fundamental mechanism promoting cortical reorganization and recovery of function.

Brain regions engaged in unilateral hand movements in monkeys and humans are found along the precentral gyrus. The primary motor cortex (M1) is located on the rostral wall of the central sulcus and corresponds to Brodmann area (BA) 4 (Brodman, 1909) or area F1 in macaques (Rizzolatti et al., 2002). M1 is supposed to be the primary origin of fiber pathways descending to the spinal cord neurons which ultimately connect to peripheral muscles (Porter and Lemon, 1993). The premotor cortex (BA 6) is situated anterior to M1 within agranular cortex and may be classified into a number of subregions based on structural and functional criteria (Graziano et al., 2002; Rizzolatti et al., 2002; Schubotz and von Cramon, 2003; Tokuno and Tanji, 1993). The premotor cortex within the interhemispheric fissure hosts the supplementary motor area (SMA, macaque area F3), which is engaged in the initiation of movements and sequential movements (Dum and Strick, 2002; Jenkins et al., 2000; Passingham, 1997). Single-cell recording data showed that a large proportion of SMA neurons exclusively respond to contralateral hand movements (Kazennikov et al.,1999). Lateral parts of premotor cortex seem to be of particular relevance for the planning and execution of externally triggered movements, especially for the transformation of sensory stimuli into motor programs (Halsband et al., 1993; Johnson et al., 1996; Kawashima et al., 1994; Lutz et al., 2000). Neurons in dorsal portions of lateral PMC (dPMC) are especially active during sensorimotor transformations underlying reaching movements, whereas neurons in ventral portions (vPMC) are involved in controlling hand and finger movements (Hoshi and Tanji, 2007; Schubotz and von Cramon, 2002). Invasive tract tracing studies in macaques showed that both vPMC and SMA have extensive projections toM1 and, therefore, might play an important role in motor recovery, for example, by facilitating the motor output of M1 neurons through corticocortical projections (Dancause et al., 2005; Dum and Strick, 2005; Shimazu et al., 2004). All premotor areas also have substantial direct projections to spinal motor neurons and may directly contribute to the motor output (Dum

and Strick, 1996; He et al., 1993). Furthermore, findings in macaques provide evidence for homotopic direct transcallosal projections between M1, vPMC, and SMA (Boussaoud et al., 2005; Luppinoet al., 1993; Rouilleretal., 1994). These transcallosal projections might enable the engagement of the contralesional hemisphere into reorganization in the lesioned brain. In summary, motor areas such as SMA, vPMC, and M1 represent key motor areas underlying different aspects of planning and executing hand movements and, therefore, might play a pivotal role during cortical reorganization underlying recovery of hand motor function.

Previous studies on cortical connectivity in stroke patients have already revealed that neural coupling among these areas can be altered in the subacute or chronic stage after stroke (Grefkes et al., 2008b; Grefkes et al., 2010; Mintzopoulos et al., 2009; Sharma et al., 2009). For example, patients with pronounced motor deficits featured reduced positive connectivity within the affected (i.e., ipsilesional) hemisphere as well as enhanced inhibitory influences from M1 in the unaffected (i.e., contralesional) hemisphere to ipsilesional M1 (Grefkes et al., 2008b, 2010). However, the temporal dynamics of disturbed interactions among motor areas after stroke and their relationship to functional recovery remain to be elucidated. Longitudinal studies have shown that behavioral recovery mainly occurs during the first 3 months after symptom onset. We, therefore, investigated changes in cortical connectivity from the acute and subacute stage to the early chronic stage post-stroke. At each session, patients performed a functional magnetic resonance imaging (fMRI) task consisting of visually paced rhythmic fist closures. Dynamic causal modeling (DCM) was then used to assess effective connectivity within a bilateral network comprising SMA, vPMC, and M1 (Friston et al., 2003). According to previous connectivity studies (Grefkes et al., 2008b; Wang et al., 2010), we hypothesized that promoting influences of premotor areas onto ipsilesional M1 might be critically reduced in patients with severe motor impairments in the acute stage after stroke. Furthermore, we assumed that these influences will be re-established concomitant to motor recovery based on findings from transcranial magnetic stimulation (TMS) studies demonstrating a supportive role of premotor areas for motor function (Fridman et al., 2004; Johansen-Berg et al., 2002; O'Shea et al., 2007). We, furthermore, sought to investigate the role of contralesional M1 for motor recovery because recent studies provided conflicting evidence for both promoting and inhibitory influences on ipsilesional M1 activity (Gerloff et al., 2006; Grefkes et al., 2008b; Lotze et al., 2006; Murase et al., 2004; Nowak et al., 2008).

Methods

Subjects

The study was approved by the local ethics committee (file no. 08–082). All subjects gave informed written consent. We examined 12 in-patients (8 males; mean age: 67±9 years; Table 1) after a first-ever ischemic stroke in the left (n=5) or right (n=7) middle cerebral artery territory with lesions affecting the corticospinal tract (n=9 with pure subcortical lesions and n=3 with both subcortical and cortical lesions) (Fig. 1). None of the lesions affected the M1 hand representation or any other region included into the DCM analysis (see Connectivity analysis section for details). All patients reported right-hand dominance before stroke. Patients were selected according to the following criteria: (1) unilateral hand motor

deficit, (2) onset of symptoms within 72 hours, (3) no clinical signs of mirror movements, severe aphasia, or neglect. The first fMRI session was assessed within 72 hours (median: 2 days) after stroke (*acute stage*). All patients participated in a second assessment at 10–14 (median: 11) days post-stroke (*subacute stage*). Since two patients died during the following months, a subgroup of ten patients was tested again at 3–6 (median: 4) months post-stroke. As up to 95% of spontaneous motor improvements have been shown to occur during the first 3 months post-stroke (Duncan et al., 1992; Nakayama et al., 1994), we termed session 3 the *early chronic stage*. All patients received standard physiotherapy on the stroke unit of the Department of Neurology, University of Cologne, in the first 2 weeks after stroke. After their discharge, all patients underwent in-patient rehabilitation treatments for the following 6 to 8 weeks. A single fMRI assessment of twelve age-matched right-handed healthy participants (6 males; 62±13 years) served as reference for brain connectivity. fMRI data from healthy subjects and ten patients in the acute stage were included in a previous publication (Rehme et al., 2010). However, whereas we previously investigated longitudinal changes in neural activity in the first 2 weeks after stroke, the present study focused on changes in effective connectivity from the acute to the chronic stage. Note that all experimental procedures were identical for all sessions and subjects.

Motor performance

Three clinical scores were assessed at each session: (1) the National Institutes of Health Stroke Scale (NIHSS), (2) the Action Research Arm Test (ARAT) (Lyle, 1981) score for the affected hand, and (3) the percent grip strength of the affected relative to the unaffected hand (measured by a vigorimeter). To compute composite scores for (1) motor performance at each session and (2) motor recovery between sessions, we entered ARAT and grip force scores into factor analyses with principal component extraction (principal component analysis, PCA; Statistical Package of the Social Sciences, SPSS17). The NIHSS scores were not included into the composite motor scores because the NIHSS measures global neurological impairment whereas the ARAT and the grip force index more specifically assess motor performance of the affected hand. The PCA with ARAT and grip force indices for each session as input variables yielded a one-factor solution explaining 90% of the variance of the two variables. As both variables loaded positively on this factor (i.e., 95%), factor values for each patient were defined as *composite motor performance scores* for each session (Fig. 2A). To yield recovery scores for different time intervals (i.e., session 1–session 2, session 2–session 3, and session 1–session 3), we first computed the respective difference scores in the ARAT and the grip force indices which were then entered into three separate PCAs. Each PCA showed a one-factor solution explaining between 73% and 89% of the variance of the difference scores which loaded positively on the respective factor (i.e., 85–95%). The factor values for each patient were hence defined as *composite motor recovery scores*. Note that negative values do not imply deterioration of motor performance but poorer motor performance or less motor improvement compared to the whole group.

Magnetic resonance imaging

The fMRI motor task consisted of visually cued rhythmic fist closures performed in blocks of moving either the left or the right hand (Grefkes et al., 2008a,b; Rehme et al., 2010). fMRI pilot scans showed that this task yielded more robust and stronger blood-oxygen-level-

dependent (BOLD) signal changes as compared to finger tapping or sequential finger movements. As robust activations on single-subject level are an important prerequisite for DCM analyses, this task appeared to be most suited to investigate neural activity in stroke patients during recovery. The task was presented on a shielded thin-film transistor (TFT) screen at the rear end of the scanner which was visible via a mirror mounted to the MR head coil. Written instructions were displayed for 2 s indicating whether the left or the right hand had to be moved in the upcoming block of trials. The task consisted of 4 blocks per hand resulting in 8 blocks per session presented in a randomized sequence. Subjects were asked to perform fist closures at the frequency of a blinking circle (1 Hz) for 15 s until a black screen indicated to rest for 15 s (plus a temporal jitter of 1–2.5 s). Hence, a correct number of fist closures corresponded to 15 movements per block. Subjects were trained inside the scanner until they reached a stable performance in three successive trials. The number of fist closures per block was counted by an experimenter standing next to the scanner.

MR images were acquired on a Siemens Trio 3.0-T scanner (Siemens Medical Solutions, Erlangen, Germany). We used a gradient echo planar imaging (EPI) sequence with the following imaging parameters: TR=1630 ms, TE=30 ms, FOV=200 mm, 26 axial slices, voxel size=$3.0 \times 3.0 \times 4.0$ mm^3, flip angle=72°, volumes=176 (4 dummy images). The slices covered a region extending from the vertex to lower parts of the cerebellum. At each session, diffusion-weighted images (DWI; TR=5100 ms, TE=104 ms, FOV=230 mm, 30 axial slices, voxel size=$1.8 \times 1.8 \times 3.0$ mm^3) were acquired to assess location and extent of the ischemic lesion. In addition, we acquired high-resolution T1weighted structural images (TR=2250 ms, TE=3.93 ms, FOV= 256 mm, 176 sagittal slices, voxel size=$1.0 \times 1.0 \times 1.0$ mm^3).

Image processing

Prior to data analysis, images from patients with right-sided lesions were flipped along the midsagittal plane. Image processing was performed using Statistical Parametric Mapping (SPM8, http://www.fil.ion.ucl.ac.uk/spm/). For control group comparisons, an equal number of healthy subjects were processed in the same manner. After realignment of the EPI volumes and co-registration with the anatomical T1 image, a lesion mask was constructed from the DWI volume showing the largest lesion extent (MRIcron; www.sph.sc.edu/comd/ rorden/MRicron). All volumes were spatially normalized to the standard template of the Montreal Neurological Institute (MNI, Canada) employing the unified segmentation approach with masked lesion (Ashburner and Friston, 2005). Finally, data were smoothed using an isotropic Gaussian kernel of 8-mm full width at half maximum. For statistical analysis, box-car vectors for each condition (i.e., affected hand movement, unaffected hand movement, instruction) were convolved with a canonical hemodynamic response function (HRF) to create the regressors of interest for the general linear model (GLM). Head movement estimates were used as confound regressors. For single subject analyses, voxels were identified as significant at a threshold of T=3.14 (p<0.001). For the group analysis, first-level contrast images of patients who attended all three assessments (n=10) were entered into a full factorial random-effects analysis (Friston et al., 1999, 2002) with the within-subject factors HAND and SESSION.

Connectivity analysis

In DCM, the brain is regarded as a deterministic, dynamic input-state-output system. An important advantage of DCM over approaches such as structural equation modeling is that it does not work on the level of the fMRI signal, which is a slow and regionally inhomogeneous hemodynamic signal, but rather uses a biophysically validated hemodynamic model to decompose the measured data into underlying neuronal signal and hemodynamic effects (Friston et al., 2003). DCM, therefore, represents an advanced additional analysis for fMRI data that enables mechanistic inference on the interactions of areas of a network that drive functional activations. Moreover, DCM may actually be more robust in clinical populations than fMRI as the hemodynamic response is estimated specifically for each region (Friston et al., 2003; Stephan et al., 2007) allowing accommodating responses that are rather different from the standard canonical HRF.

In addition to the hemodynamic model, DCM estimates three sets of parameters. These are (i) endogenous coupling independent of the experimental condition (DCM A-matrix); (ii) parameters for context-dependent changes in coupling evoked by the experimental conditions, that is, changes in effective connectivity between two regions caused by the current task (DCM B-matrix); and (iii) the direct experimental input to the system that drive regional activity (DCM C-matrix). DCM is a hypothesis-driven approach to model effective connectivity between distinct regions where models are fitted to subject-specific regional fMRI time series (Friston et al., 2003). Therefore, we extracted the first eigenvariate of the effects-of-interest adjusted time series from all voxels within 8-mm spheres around local activation maxima of eight regions of interest. Local activation maxima were identified on the normalized SPMs of each subject and session. Regions of interest consisted of M1, SMA, and ventral PMC representing core regions of the cortical motor system engaged in fist closure movements (Eickhoff et al., 2008; Grefkes et al., 2008b). Furthermore, the primary visual cortex (V1) was defined as sensory input region as hand movements were triggered by a blinking visual cue. As individual activation maxima may vary across subjects (Eickhoff et al., 2009), we ensured comparability by selecting coordinates according to the following anatomical constraints: M1 on the rostral wall of the central sulcus at the "hand knob" formation, SMA on the mesial wall within the interhemispheric fissure between the paracentral lobule (posterior landmark) and the plane running through the anterior commissure ($y<0$), superior vPMC situated in the precentral sulcus at the level of the inferior frontal sulcus ($z<51$) (Tomassini et al., 2007), and the primary visual cortex (V1) within the calcarine sulcus. None of the patients had a lesion in one of these regions as reviewed by a neurologist (CG). Coordinates were defined for baseline contrasts at a threshold of $p<0.001$ uncorrected (i.e., left M1/SMA/PMC in the contrast for movements of the affected hand; right M1/SMA/PMC in the contrast for movements of the unaffected hand). V1 coordinates were specified from a conjunction analysis across both conditions. As the location of maximum activation may also vary between sessions, a dispersion of coordinates up to 8 mm, which is equivalent to the spatial smoothing kernel, was allowed between sessions to warrant within-subject consistency of anatomical areas. If there was no activation within 8 mm at $p<0.001$, the statistical threshold was lowered to $p<0.05$ uncorrected. This was the case in two patients.

Based on structural connectivity data derived from invasive studies in macaque monkeys, we assumed endogenous connections (DCM A-matrix) between SMA and ipsilateral and contralateral M1 (Rouiller et al., 1994), between SMA and ipsilateral (Luppino et al., 1993) as well as contralateral PMC (Boussaoud et al., 2005), between PMC and both ipsi- and contralateral M1 (Rouiller et al., 1994), as well as homotopic transcallosal connections between M1–M1 (Rouiller et al., 1994), SMA–SMA (McGuire et al., 1991; Rouiller et al., 1994), and PMC–PMC (Boussaoud et al., 2005). As hand movements were triggered by a blinking visual cue, we assumed that activity in premotor areas (SMA, PMC) was driven by visual cortex activity (V1) (Fig. 3). Importantly, coupling parameters obtained from DCM refer to functional interactions but do not necessarily reflect direct axonal connections. While all the abovementioned areas represent key nodes of the cortical motor network, it should be noted that other brain regions may also contribute to task performance (e.g., cerebellar areas, basal ganglia, and frontoparietal areas). Furthermore, the relay of neural information by regions which were not explicitly modelled in DCM is implicitly captured in the coupling parameters between two regions (Friston et al., 2003; Stephan et al., 2010).

Bayesian model selection

Condition-specific modulations of interregional coupling may not necessarily affect all endogenous anatomical connections (Penny et al., 2004; Stephan et al., 2009). Based on the endogenous connectivity matrix (DCM A-matrix), we set up 17 alternative models of connectivity representing biologically plausible hypotheses on interregional coupling among regions of interest during the performance of left and right fist closures (DCM B-matrix). As the task was visually triggered, V1 was supposed to be directly driven by task-dependent influences (DCM C-matrix). Starting from a fully connected DCM B-matrix, we constructed 17 models according to (i) the presence of interhemispheric connections and (ii) the lateralization of coupling towards M1 contralateral to the moving hand (Supplementary Fig. 1). At first, we omitted heterotopic interhemispheric connections between premotor areas and M1 (models 2–5), then we removed homotopic connections between motor areas (i.e., SMA–SMA, PMC–PMC, M1–M1) (models 6–8). Finally, all interhemispheric connections were removed (model 9). Afterwards, the same approach was applied to lateralized models which contained connections only to M1 contralateral to the moving hand. We then applied Bayesian model selection (BMS) random-effects analysis to determine the most likely model given the data (Stephan et al., 2009).

Statistical analysis

The statistical analyses were carried out based on classical inference using analyses of variance (ANOVAs) and *t*-tests. Note that the arithmetic mean of each parameter closely approximated the averaged mean of the posterior distribution weighted by the averaged posterior covariances for each group and session. Therefore, group differences and longitudinal changes in averaged posterior means showed a similar pattern of results as the classical approach. Statistical significance of the derived coupling parameters for all 30 connections of the most likely DCM was tested by means of one-sample *t*-tests for each session ($p<0.05$ false discovery rate (FDR)-corrected for multiple comparisons) (Benjamini and Hochberg, 1995). For comparisons between groups (between-subject factor GROUP, levels patients, controls), coupling parameters for all 30 connections (within-subject factor

CONNECTION) were entered into a mixed-design ANOVA for each session. Significant interaction effects between GROUP and CONNECTION were followed up by comparisons between patients and control subjects in all 30 connections. The significance level of $p<0.05$ was corrected for the number of these 30 follow-up comparisons (Dunn, 1961). Coupling parameters which were significantly enhanced or reduced in patients compared to controls were then analyzed between sessions within the patients' group using paired t-tests for different time periods (i.e., session 1–session 2 [n=12 patients], session 1–session 3 [n=10 patients], and session 2–session 3 [n=10 patients]).

Correlation with motor performance and motor recovery

To investigate the relationship between abnormally altered coupling parameters and motor behavior, we computed Pearson's correlations between coupling parameters of those connections, which showed significant differences compared to healthy controls, and the composite motor performance scores. In addition, significant changes in coupling parameters over time were correlated with the composite motor recovery scores. The significance threshold was defined at $p<0.05$ one-tailed because we assumed a unidirectional relationship, that is, the more pronounced the impairment the bigger the reduction in (positive or negative) coupling strength and the greater the amount of recovery the stronger the increases in coupling strength.

Prediction of motor performance and motor recovery

To identify coupling parameters that correlated with recovery and outcome at later stages, significantly altered coupling parameters as well as significant changes across sessions were correlated with the composite motor performance scores at (i) session 2 and (ii) session 3 as well as with composite motor recovery scores between (iii) session 1–session 2 and (iv) session 1–session 3.

Results

Behavioral and fMRI results

A repeated-measures ANOVA on composite motor performance scores at session 1 and session 2 showed a significant main effect of SESSION ($F(1,11)$=10.560, p=0.008) indicating significant improvements from the acute to the subacute phase (Fig. 2A). An ANOVA on composite motor performance scores for all three sessions showed a trend towards significance ($F(2,18)$=2.959, p=0.077). Hence, the greatest amount of recovery seemed to occur within the first 2 weeks.

The fMRI results from healthy subjects and the group of 10 patients who attended all 3 sessions are shown in Fig. 2B and C. In healthy subjects, right or left fist closures increased the BOLD signal in a network comprising contralateral M1, SMA, dPMC and vPMC, postcentral gyrus (primary somatosensory cortex, S1), bilateral parietal operculum (secondary somatosensory cortex, S2) and frontal operculum, putamen and thalamus, and ipsilateral cerebellum. In patients, movements of the unaffected hand revealed similar activations as left- or right-hand movements in healthy subjects. Movements of the stroke-affected hand were associated with additional BOLD signal increases in the ipsilateral (i.e.,

contralesional) hemisphere with clusters of activation in dPMC and vPMC, S1, and M1 which was most pronounced at session 2 (i.e., 10–14 days post-stroke).

BMS random-effects analysis

Model 1 representing a fully connected DCM B-matrix for movements of the left or right hand showed the best model fit across groups and sessions (Fig. 3; Supplementary Fig. 1). Expected posterior and exceedance probabilities are given in Supplementary Fig. 2. In summary, for the respective populations the subjects were drawn from, model 1 had a probability of 35–97% for being the most likely generative model given the observed data. The BMS analysis revealed similar results for healthy subjects and the patients' group at sessions 2 and 3 as well as across all three sessions of the patients' group.

Effective connectivity

Coupling parameters representing the coupling strength from one area over another correspond to rates in Hz (1/s). Positive coupling rates indicate that the source region exerts a promoting influence on the activity of the target area. Negative coupling rates indicate that the source region exerts a negative or inhibitory effect on the activity of a target region (Friston et al., 2003).

We focused our analysis on the coupling among areas in the context of affected hand movements (DCM B-matrix). Coupling estimates for movements of the unaffected hand (left hand in controls) were not different between patients and controls (mixed-design ANOVA, $p>0.05$) and did not change across time post-stroke (repeated-measures ANOVA, $p>0.05$). The analysis of endogenous coupling parameters (DCM A-matrix), which denote the neural coupling between areas independent of the effect of the task, yielded similar results as found for the modulatory influence during movements of the affected hand. Hence, these results are reported in the supplementary material (Supplementary text; Supplementary Fig. 3; Supplementary Tables 1 and 2).

Coupling parameters at sessions 1 and 2 were not significantly different between the whole group ($n=12$) and the subgroup of patients who attended all three assessments ($n=10$). Hence, results from 12 patients are reported for the first two sessions to increase the sensitivity of our analysis.

Changes in the ipsilesional hemisphere

At session 1 (72 hours post-stroke), coupling parameters for movements of the affected hand (right hand for controls) showed a significant interaction effect between GROUP and CONNECTION ($F(29,638)=5.874$, $p<0.001$). Positive influences from ipsilesional SMA and bilateral PMC onto ipsilesional M1 were significantly reduced compared to healthy controls ($p<0.05$ corrected for multiple comparisons; Table 2, Fig. 4A) and correlated positively with the composite motor performance scores at session 1. Hence, patients with more severe motor impairments showed a stronger reduction of positive influences from ipsilesional and contralesional premotor areas on ipsilesional M1 relative to controls (Fig. 4B). Importantly, these results remained significant after the exclusion of two patients who were not able to perform the requested number of fist closures in the scanner at the first session.

At session 2 (10–14 days post-stroke), the interaction between GROUP and CONNECTION was again significant ($F_{(29,638)}$=2.647, p<0.001; Table 2). Positive coupling of ipsilesional SMA with ipsilesional M1 remained significantly reduced. The repeated-measures ANOVA showed no significant differences compared to healthy subjects at session 3 (3–6 months post-stroke).

The coupling strength between SMA and M1 in the ipsilesional hemisphere increased significantly within 2 weeks (t(11)=2.404, p=0.035) as well as across the whole time period (t(9)=2.682, p=0.025). This significant increase correlated positively with the composite motor recovery score (Fig. 5A, B, C; Table 3).

In summary, the modulation of neural coupling during movements of the affected hand showed significantly weaker interactions between ipsilesional premotor areas and ipsilesional M1 early after stroke, particularly in patients with more severe initial impairment. Positive coupling towards ipsilesional M1 increased concomitant to motor recovery towards levels observed among healthy participants.

Changes in the contralesional hemisphere

Post hoc tests for the significant interaction between GROUP and CONNECTION at session 1 (see above) also revealed attenuated negative influences from ipsilesional M1 to contralesional M1 as compared to controls, especially in severely affected patients (p<0.05 corrected for multiple comparisons; Fig. 4A; Table 2). Furthermore, the negative coupling from ipsilesional SMA and ipsilesional PMC on contralesional M1 was significantly reduced. Again, results for the contralesional hemisphere remained unchanged after the exclusion of two patients who were not able to perform the requested number of fist closures in the scanner at session 1.

At session 2, follow-up tests for the interaction between GROUP and CONNECTION showed that negative coupling from ipsilesional M1, SMA, and PMC towards contralesional M1 remained significantly reduced relative to healthy controls. Importantly, patients now showed an additional positive influence from contralesional onto ipsilesional M1 which was not present in healthy subjects and which correlated negatively with the composite motor performance scores. At session 3, there was no significant difference in neural coupling between patients and healthy subjects.

Negative coupling from ipsilesional SMA and ipsilesional PMC towards contralesional M1 increased from sessions 2 to 3 towards levels observed in healthy subjects (t(9)=3.668, p=0.005; t(9)= 3.159, p=0.012). Furthermore, parameters for the interhemispheric coupling from ipsilesional on contralesional M1 increased steadily from session 1 to session 3 (t(9)=3.350, p=0.009). Across the whole group, the additional positive coupling between contralesional M1 and ipsilesional M1 significantly decreased to zero between sessions 2 and 3 (t(9)=3.675, p=0.005; Fig. 5D; Table 3), and resembled levels observed in healthy controls.

In summary, we observed reduced inhibitory coupling from ipsilesional M1 and SMA to contralesional M1 after 2 weeks. At the same time, there was a positive, promoting influence

from contralesional to ipsilesional M1, especially in patients with poor motor performance. The transition from the subacute to the early chronic stage was characterized by a reinstatement of inhibitory influences of ipsilesional areas on contralesional M1 activity.

Prediction of motor performance and motor recovery

The *composite motor performance score* at session 2 correlated positively with the coupling strength from ipsilesional SMA and PMC towards ipsilesional M1 at session 1 (Fig. 6A). The composite motor performance score at session 3 correlated positively with an increase in coupling from contralesional to ipsilesional M1from sessions 2 to 3.This means that patients who developed strong negative influences originating from contralesional M1 showed a relatively poorer outcome as compared to patients featuring a positive coupling (Fig. 6B).

The *composite motor recovery score* computed between sessions 1 and 2 correlated negatively with coupling estimates from ipsilesional SMA and PMC to ipsilesional M1 at session 1 (Fig. 6C). Hence, reduced positive influences towards ipsilesional M1 predicted a greater amount of recovery within the first 2 weeks post-stroke. Similarly, the composite motor recovery score between sessions 1 and 3 correlated negatively with the connection strength from ipsilesional SMA and PMC to M1 at session 1 (Fig. 6D).

In summary, motor recovery and motor performance in the subacute and early chronic stage depended upon the strength of positive influences from ipsilesional premotor areas onto ipsilesional M1. In contrast, motor performance in the early chronic stage was also determined by the influences exerted by contralesional M1.

Discussion

Spontaneous recovery from stroke-induced motor deficits typically occurs during the first 30 days up to 3 months after symptom onset (Duncan et al., 1992; Nakayama et al., 1994). For this early post-stroke period, results from longitudinal fMRI studies in humans and rats showed that neural activity in ipsilesional sensorimotor cortex recovers whereas abnormally enhanced BOLD activity in contralesional sensorimotor areas decreases concomitant to behavioral improvements (Dijkhuizen et al., 2001; Dijkhuizen et al., 2003; Loubinoux et al., 2003; Tombari et al., 2004; Ward et al., 2003; Weber et al., 2008). In the present study, the modeling of underlying neural responses from fMRI time series using DCM revealed disturbed neural coupling among motor areas of both hemispheres which provides an explanation for altered BOLD activity patterns after stroke and recovery of function over time (Fig. 4).

Reorganization in the ipsilesional hemisphere

Our results together with previous DCM findings in chronic stroke patients (Grefkes et al., 2008b; 2010; Sharma et al., 2009) suggest that impaired motor performance early after stroke is influenced by abnormally weak neural coupling between higher order premotor areas as well as between premotor areas and ipsilesional M1. The relationship between ipsilesional M1 connectivity and motor recovery after stroke was also addressed by a recent longitudinal study using graph theoretical approaches (Wang et al., 2010). Here, motor

recovery was associated with an increase in information processing mediated by ipsilesional M1. Findings from other fMRI studies suggested that stronger BOLD signal in ipsilesional M1 and SMA predicts a higher level of recovery at later stages (Loubinoux et al., 2003; Loubinoux et al., 2007). We show here that also the coupling strength among these areas determines clinical outcome. Hence, the relationship between increases in ipsilesional SMA–M1 coupling and motor improvements suggests a supportive role of premotor areas for motor recovery up to the early chronic stage. However, neural coupling from bilateral premotor areas onto ipsilesional M1 did not exceed levels observed in healthy subjects indicating that recovery-related increases do not compensate for stroke-induced disturbances of the motor network but rather reflect a normalization of neural coupling. The account of a supportive role of ipsilesional premotor areas is confirmed by TMS studies showing that a disruption of ipsilesional dPMC activity leads to a deterioration of recovered motor function of the paretic hand (Fridman et al., 2004). Similarly, TMSinduced disruption of dPMC activity ipsilateral to the moving hand of healthy subjects (corresponding to the contralesional hemisphere in patients) impairs motor performance (O'Shea et al., 2007). This finding provides evidence for a compensatory role of dPMC. Our data show that the coupling between contralesional vPMC and ipsilesional M1 was significantly reduced in the acute stage but did not correlate with motor performance. This interhemispheric PMC–M1 coupling subsequently returned towards levels observed in healthy subjects in the early chronic stage. Hence, our results show that the "dysconnectivity" of ipsilesional M1 in the acute stage not only includes reduced coupling with ipsilesional PMC and SMA but also reduced coupling with premotor areas of the unaffected hemisphere.

Reorganization in the contralesional hemisphere

The role of the unaffected hemisphere in cortical reorganization after stroke is still highly controversial (Bütefisch et al., 2005; Chollet et al., 1991; Fridman et al., 2004; Gerloff et al., 2006; Weiller et al., 1992). TMS studies on interhemispheric inhibition suggested that contralesional M1 exerts enhanced inhibitory influences on ipsilesional M1 in some patients, thereby contributing to the motor deficit (Duque et al., 2005; Murase et al., 2004). In contrast, fMRI studies investigating resting state functional connectivity of the sensorimotor system provided evidence for a supportive role of the interhemispheric functional connectivity between sensorimotor cortices (Carter et al., 2010; van Meer et al., 2010). Van Meer et al. (2010) found that impaired motor performance in the first days after experimental stroke in rats was associated with a reduction of interhemispheric functional connectivity. Interhemispheric connectivity increased subsequently concomitant to sensorimotor improvements. These results are in accordance with findings of Carter et al. (2010) in human stroke patients. Here, the level of interhemispheric connectivity between homologous regions of the motor system correlated positively with motor performance whereas connectivity in the ipsilesional hemisphere was not related to behavior. Similar to the evidence provided by these functional connectivity studies, our data demonstrate that particularly patients with more severe motor impairments may benefit from an additional positive influence from contralesional onto ipsilesional M1 within 2 weeks after stroke (Fig. 4). This finding suggests that contralesional M1 activity promotes the function of ipsilesional M1. At first sight, these results seem at odds with the results of Grefkes et al. (2008b) showing that contralesional M1 exerted additional inhibitory influences on

ipsilesional M1 in patients with incomplete motor recovery at the chronic stage post-stroke. However, different neural mechanisms may underlie changes of effective connectivity in the acute and chronic stage. A longitudinal fMRI study investigating recovery from aphasia also reported a transient upregulation of neural activity in homologous contralesional areas concomitant to language improvements (Saur et al., 2006). In line with this finding, we observed that inhibitory neural coupling from premotor areas onto contralesional M1 normalized between the subacute and the early chronic stage suggesting a re-inhibition of contralesional M1activity concomitant to steady increases of promoting influences within the ipsilesional motor network. Furthermore, this normalization of neural coupling from contralesional to ipsilesional M1 was predictive for the behavioral outcome at the early chronic stage (Fig. 6B): patients with relatively poorer motor performance now featured enhanced inhibitory contralesional–ipsilesional M1 coupling. Note that in contrast to the study of Grefkes et al. (2008b), our group of patients showed milder levels of impairment after 3–6 months (Table 1). This might explain why we found abnormal inhibitory contralesional–ipsilesional M1 coupling only in patients who maintained stronger motor impairments. One speculation is that contralesional M1 activity initially supports the restitution of the ipsilesional motor network, whereas a persistent influence of contralesional M1 in the chronic stage might turn into enhanced inhibitory coupling indicating a negative influence on neural processing in the ipsilesional hemisphere. Such a conclusion is in line with non-invasive intervention studies which showed that reducing excitability of the contralesional M1 by means of repetitive TMS or transcranial direct current stimulation (tDCS) improves motor functions of the paretic hand (Grefkes et al., 2010; Hummel and Cohen, 2006; Nowak et al., 2008).

Limitations and conclusion

One limitation of the present study pertains to the low number of subjects. However, despite the small sample size, we found significant alterations in effective connectivity as compared to healthy subjects. Nevertheless, data from larger samples might have been more sensitive for even smaller differences between patients and controls. Furthermore, differential effects of factors such as the difference between left- or right-sided lesions or the anatomical location of structural damage on effective connectivity could be better addressed in studies with more extended cohorts.

Another limitation of the present study is that the BOLD signal could be altered in stroke patients due to vascular disease. However, Weber et al. (2008) reported evidence for a preserved coupling of the hemodynamic BOLD signal and neuronal activity after stroke in rats. None of our patients suffered from a significant artery occlusion causing reductions in blood flow. In addition, lesions were usually focal and mostly located in subcortical structures (Fig. 1) and changes in BOLD activity were also observed in the undamaged hemisphere (Fig. 2). Most importantly, in clinical populations DCM may actually be more robust than standard GLM analyses using a canonical HRF as the hemodynamic response is estimated specifically for each region (Friston et al., 2003; Stephan et al., 2007). However, some biophysiological and neurovascular processes are neglected in the current DCM implementation, probably because they may not be easily identified from fMRI data (Daunizeau et al., 2009). Nevertheless, DCM has been validated by simulation and

experimental studies in humans and animals (David et al., 2008a, 2008b; Moran et al., 2008). Importantly, the studies of David et al. (2008ab) provide evidence for the validity of DCM for inferring network structure from fMRI data using simultaneous fMRI and electroencephalography (EEG) measurements in rodents with epileptic seizures.

The current study showed that the restitution of connectivity among ipsilesional areas constitutes an important predictor for motor recovery. As the sample size was rather small, results of this study alone may be insufficient to resolve the contradictions in the literature regarding the potential role of contralesional M1 in recovery after stroke. However, the role of contralesional M1 seems to depend on the factor time since stroke. Therefore, our data suggest that interventions aiming at a reduction of contralesional M1 activity have to be considered with caution early after stroke but may be useful in patients with persistent motor deficits at the chronic stage to reduce abnormally enhanced inhibitory M1–M1 coupling.

Supplementary materials related to this article can be found online at doi:10.1016/j.neuroimage.2011.01.014.

Supplementary Material

Refer to Web version on PubMed Central for supplementary material.

Acknowledgments

References

Ashburner J, Friston K, 2005. Unified segmentation. Neuroimage 26, 839–851. [PubMed: 15955494]

Benjamini Y, Hochberg Y, 1995. Controlling the false discovery rate: a practical and powerful approach to multiple testing. J. R. Stat. Soc. B 57.

Boussaoud D, Tanne-Gariepy J, Wannier T, Rouiller EM, 2005. Callosal connections of dorsal versus ventral premotor areas in the macaque monkey: a multiple retrograde tracing study. BMC Neurosci. 6, 67. [PubMed: 16309550]

Brodman K, 1909. Vergleichende Lokalisationslehre der Grosshirnrinde in ihren Prinzipien dargestellt auf Grund des Zellenbaues. Barth, Leipzig.

Bütefisch CM, Kleiser R, Müller K, Wittsack HJ, Hömberg V, Seitz RJ, 2005. Recruitment of contralesional motor cortex in stroke patients with recovery of hand function. Neurology 64, 1067–1069. [PubMed: 15781831]

Carter AR, Astafiev SV, Lang CE, Connor LT, Rengachary J, Strube MJ, Pope DLW, Shulman GL, Corbetta M, 2010. Resting interhemispheric functional magnetic resonance imaging connectivity predicts performance after stroke. Ann. Neurol 67, 365–375. [PubMed: 20373348]

Chollet F, DiPiero V, Wise RJ, Brooks DJ, Dolan RJ, Frackowiak RS, 1991. The functional anatomy of motor recovery after stroke in humans: a study with positron emission tomography. Ann. Neurol 29, 63–71. [PubMed: 1996881]

Dancause N, Barbay S, Frost SB, Plautz EJ, Chen D, Zoubina EV, Stowe AM, Nudo RJ, 2005. Extensive cortical rewiring after brain injury. J. Neurosci 25, 10167–10179. [PubMed: 16267224]

Daunizeau J, David O, Stephan KE, 2009. Dynamic causal modelling: a critical review of the biophysical and statistical foundations. Neuroimage (doi:10.1016).

David O, Guillemain I, Saillet S, Reyt S, Deransart C, Segebarth C, Depaulis A, 2008a. Identifying neural drivers with functional MRI: an electrophysiological validation. PLoS Biol. 6, 2683–2697. [PubMed: 19108604]

David O, Wozniak A, Minotti L, Kahane P, 2008b. Preictal short-term plasticity induced by intracerebral 1 Hz stimulation. Neuroimage 39, 1633–1646. [PubMed: 18155929]

Dijkhuizen RM, Ren J, Mandeville JB, Wu O, Ozdag FM, Moskowitz MA, Rosen BR, Finklestein SP, 2001. Functional magnetic resonance imaging of reorganization in rat brain after stroke. Proc. Natl. Acad. Sci. U. S. A 98, 12766–12771. [PubMed: 11606760]

Dijkhuizen RM, Singhal AB, Mandeville JB, Wu O, Halpern EF, Finklestein SP, Rosen BR, Lo EH, 2003. Correlation between brain reorganization, ischemic damage, and neurologic status after transient focal cerebral ischemia in rats: a functional magnetic resonance imaging study. J. Neurosci 23, 510–517. [PubMed: 12533611]

Dum RP, Strick PL, 1996. Spinal cord terminations of the medial wall motor areas in macaque monkeys. J. Neurosci 16, 6513–6525. [PubMed: 8815929]

Dum RP, Strick PL, 2002. Motor areas in the frontal lobe of the primate. Physiol. Behav 77, 677–682. [PubMed: 12527018]

Dum RP, Strick PL, 2005. Frontal lobe inputs to the digit representations of the motor areas on the lateral surface of the hemisphere. J. Neurosci 25, 1375–1386. [PubMed: 15703391]

Duncan PW, Goldstein LB, Matchar D, Divine GW, Feussner J, 1992. Measurement of motor recovery after stroke. Outcome assessment and sample size requirements. Stroke 23, 1084–1089. [PubMed: 1636182]

Dunn OJ, 1961. Multiple comparison among means. J. Am. Stat. Assoc 56, 52–64.

Duque J, Hummel F, Celnik P, Murase N, Mazzocchio R, Cohen LG, 2005. Transcallosal inhibition in chronic subcortical stroke. Neuroimage 28, 940–946. [PubMed: 16084737]

Eickhoff SB, Dafotakis M, Grefkes C, Shah NJ, Zilles K, Piza-Katzer H, 2008. Central adaptation following heterotopic hand replantation probed by fMRI and effective connectivity analysis. Exp. Neurol 212, 132–144. [PubMed: 18501895]

Eickhoff SB, Heim S, Zilles K, Amunts K, 2009. A systems perspective on the effective connectivity of overt speech production. Philos. Transact. A Math. Phys Eng. Sci 367, 2399–2421.

Fridman EA, Hanakawa T, Chung M, Hummel F, Leiguarda R, Cohen LG, 2004. Reorganization of human premotor cortex after stroke recovery. Brain 127, 747–758. [PubMed: 14749291]

Friston KJ, Holmes AP, Price CJ, Buchel C, Worsley KJ, 1999. Multisubject fMRI studies and conjunction analyses. Neuroimage 10, 385–396. [PubMed: 10493897]

Friston KJ, Glaser DE, Henson RN, Kiebel S, Phillips C, Ashburner J, 2002. Classical and Bayesian inference in neuroimaging: applications. Neuroimage 16, 484–512. [PubMed: 12030833]

Friston KJ, Harrison L, Penny W, 2003. Dynamic causal modelling. Neuroimage 19, 1273–1302. [PubMed: 12948688]

Gerloff C, Bushara K, Sailer A, Wassermann EM, Chen R, Matsuoka T, Waldvogel D, Wittenberg GF, Ishii K, Cohen LG, Hallett M, 2006. Multimodal imaging of brain reorganization in motor areas of the contralesional hemisphere of well recovered patients after capsular stroke. Brain 129, 791–808. [PubMed: 16364955]

Graziano MS, Taylor CS, Moore T, Cooke DF, 2002. The cortical control of movement revisited. Neuron 36, 349–362. [PubMed: 12408840]

Grefkes C, Eickhoff SB, Nowak DA, Dafotakis M, Fink GR, 2008a. Dynamic intra- and interhemispheric interactions during unilateral and bilateral hand movements assessed with fMRI and DCM. Neuroimage 41, 1382–1394. [PubMed: 18486490]

Grefkes C, Nowak DA, Eickhoff SB, Dafotakis M, Kust J, Karbe H, Fink GR, 2008b. Cortical connectivity after subcortical stroke assessed with functional magnetic resonance imaging. Ann. Neurol 63, 236–246. [PubMed: 17896791]

Grefkes C, Nowak DA, Wang LE, Dafotakis M, Eickhoff SB, Fink GR, 2010. Modulating cortical connectivity in stroke patients by rTMS assessed with fMRI and dynamic causal modeling. Neuroimage 50, 233–242. [PubMed: 20005962]

Halsband U, Ito N, Tanji J, Freund HJ, 1993. The role of premotor cortex and the supplementary motor area in the temporal control of movement in man. Brain 116, 243–266. [PubMed: 8453461]

He SQ, Dum RP, Strick PL, 1993. Topographic organization of corticospinal projections from the frontal lobe: motor areas on the lateral surface of the hemisphere. J. Neurosci 13, 952–980. [PubMed: 7680069]

Hoshi E, Tanji J, 2007. Distinctions between dorsal and ventral premotor areas: anatomical connectivity and functional properties. Curr. Opin. Neurobiol17, 234–242. [PubMed: 17317152]

Hummel FC, Cohen LG, 2006. Non-invasive brain stimulation: a new strategy to improve neurorehabilitation after stroke? Lancet Neurol. 5, 708–712. [PubMed: 16857577]

Jenkins IH, Jahanshahi M, Jueptner M, Passingham RE, Brooks DJ, 2000. Self-initiated versus externally triggered movements. II. The effect of movement predictability on regional cerebral blood flow. Brain 123, 1216–1228. [PubMed: 10825359]

Johansen-Berg H, Rushworth MF, Bogdanovic MD, Kischka U, Wimalaratna S, Matthews PM, 2002. The role of ipsilateral premotor cortex in hand movement after stroke. Proc. Natl. Acad. Sci. U. S. A 99, 14518–14523. [PubMed: 12376621]

Johnson PB, Ferraina S, Bianchi L, Caminiti R, 1996. Cortical networks for visual reaching: physiological and anatomical organization of frontal and parietal lobe arm regions. Cereb. Cortex 6, 102–119. [PubMed: 8670643]

Kawashima R, Roland PE, O'Sullivan BT, 1994. Fields in human motor areas involved in preparation for reaching, actual reaching, and visuomotor learning: a positron emission tomography study. J. Neurosci 14, 3462–3474. [PubMed: 8207466]

Kazennikov O, Hyland B, Corboz M, Babalian A, Rouiller EM, Wiesendanger M, 1999. Neural activity of supplementary and primary motor areas in monkeys and its relation to bimanual and unimanual movement sequences. Neuroscience 89, 661–674. [PubMed: 10199603]

Lotze M, Markert J, Sauseng P, Hoppe J, Plewnia C, Gerloff C, 2006. The role of multiple contralesional motor areas for complex hand movements after internal capsular lesion. J. Neurosci 26, 6096–6102. [PubMed: 16738254]

Loubinoux I, Carel C, Pariente J, Dechaumont S, Albucher JF, Marque P, Manelfe C, Chollet F, 2003. Correlation between cerebral reorganization and motor recovery after subcortical infarcts. Neuroimage 20, 2166–2180. [PubMed: 14683720]

Loubinoux I, Dechaumont S, Castel-Lacanal E, De Boissezon X, Marque P, Pariente J, Albucher JF, Berry I, Chollet F, 2007. Prognostic value of fMRI in recovery of hand function in subcortical stroke patients. Cereb. Cortex 17, 2980–2987. [PubMed: 17389628]

Luppino G, Matelli M, Camarda R, Rizzolatti G, 1993. Corticocortical connections of area F3 (SMA-proper) and area F6 (pre-SMA) in the macaque monkey. J. Comp. Neurol 338, 114–140. [PubMed: 7507940]

Lutz K, Specht K, Shah NJ, Jancke L,2000. Tappingmovements according toregular and irregular visual timing signals investigated with fMRI. NeuroReport 11, 1301–1306. [PubMed: 10817611]

Lyle RC, 1981. A performance test for assessment of upper limb function in physical rehabilitation treatment and research. Int. J. Rehabil. Res 4, 483–492. [PubMed: 7333761]

McGuire PK, Bates JF, Goldman-Rakic PS, 1991. Interhemispheric integration: I. Symmetry and convergence of the corticocortical connections of the left and the right supplementary motor area (SMA) in the rhesus monkey. Cereb. Cortex 1, 390–407. [PubMed: 1726605]

Mintzopoulos D, Astrakas LG, Khanicheh A, Konstas AA, Singhal A, Moskowitz MA, Rosen BR, Tzika AA, 2009. Connectivity alterations assessed by combining fMRI and MR-compatible hand robots in chronic stroke. Neuroimage 47 (Suppl 2), T90–T97. [PubMed: 19286464]

Moran RJ, Stephan KE, Kiebel SJ, Rombach N, O'Connor WT, Murphy KJ, Reilly RB, Friston KJ, 2008. Bayesian estimation of synaptic physiology from the spectral responses of neural masses. Neuroimage 42, 272–284. [PubMed: 18515149]

Murase N, Duque J, Mazzocchio R, Cohen LG, 2004. Influence of interhemispheric interactions on motor function in chronic stroke. Ann. Neurol 55, 400–409. [PubMed: 14991818]

Nakayama H, Jorgensen HS, Raaschou HO, Olsen TS, 1994. Recovery of upper extremity function in stroke patients: the Copenhagen Stroke Study. Arch. Phys. Med. Rehabil 75, 394–398. [PubMed: 8172497]

Nowak DA, Grefkes C, Dafotakis M, Eickhoff S, Kust J, Karbe H, Fink GR, 2008. Effects of low-frequency repetitive transcranial magnetic stimulation of the contralesional primary motor cortex

on movement kinematics and neural activity in subcortical stroke. Arch. Neurol 65, 741–747. [PubMed: 18541794]

O'Shea J, Johansen-Berg H, Trief D, Gobel S, Rushworth MF, 2007. Functionally specific reorganization in human premotor cortex. Neuron 54, 479–490. [PubMed: 17481399]

Passingham RE, 1997. Functional organisation of the motor system. In: Frackowiak RSJ, Friston KJ, Frith CD, Dolan RJ, Mazziotta JC (Eds.), Human Brain Function. Academic Press, San Diego, pp. 243–274.

Penny WD, Stephan KE, Mechelli A, Friston KJ, 2004. Comparing dynamic causal models. Neuroimage 22, 1157–1172. [PubMed: 15219588]

Porter R, Lemon RN, 1993. Corticospinal Neurons and Voluntary Movement. Oxford University Press, Oxford.

Rehme AK, Fink GR, von Cramon DY, Grefkes C, 2010. The role of the contralesional motor cortex for motor recovery in the early days after stroke assessed with longitudinal fMRI. Cereb. Cortex (doi:10.1093).

Rizzolatti G, Fogassi L, Gallese V, 2002. Motor and cognitive functions of the ventral premotor cortex. Curr. Opin. Neurobiol 12, 149–154. [PubMed: 12015230]

Rouiller EM, Babalian A, Kazennikov O, Moret V, Yu XH, Wiesendanger M, 1994. Transcallosal connections of the distal forelimb representations of the primary and supplementary motor cortical areas in macaque monkeys. Exp. Brain Res 102, 227–243. [PubMed: 7705502]

Saur D, Lange R, Baumgaertner A, Schraknepper V, Willmes K, Rijntjes M, Weiller C, 2006. Dynamics of language reorganization after stroke. Brain 129, 1371–1384. [PubMed: 16638796]

Schubotz RI, von Cramon DY, 2002. Predicting perceptual events activates corresponding motor schemes in lateral premotor cortex: an fMRI study. Neuroimage 15, 787–796. [PubMed: 11906220]

Schubotz RI, von Cramon DY, 2003. Functional–anatomical concepts of human premotor cortex: evidence from fMRI and PET studies. Neuroimage 20 (Suppl 1), S120–S131. [PubMed: 14597305]

Sharma N, Baron JC, Rowe JB, 2009. Motor imagery after stroke: relating outcome to motor network connectivity. Ann. Neurol 66, 604–616. [PubMed: 19938103]

Shimazu H, Maier MA, Cerri G, Kirkwood PA, Lemon RN, 2004. Macaque ventral premotor cortex exerts powerful facilitation of motor cortex outputs to upper limb motoneurons. J. Neurosci 24, 1200–1211. [PubMed: 14762138]

Stephan KE, Harrison LM, Kiebel SJ, David O, Penny WD, Friston KJ, 2007. Dynamic causal models of neural system dynamics: current state and future extensions. J. Biosci 32, 129–144. [PubMed: 17426386]

Stephan KE, Penny WD, Daunizeau J, Moran RJ, Friston KJ, 2009. Bayesian model selection for group studies. Neuroimage 46, 1004–1017. [PubMed: 19306932]

Stephan KE, Penny WD, Moran RJ, den Ouden HE, Daunizeau J, Friston KJ, 2010. Ten simple rules for dynamic causal modeling. Neuroimage 49, 3099–3109. [PubMed: 19914382]

Tokuno H, Tanji J, 1993. Input organization of distal and proximal forelimb areas in the monkey primary motor cortex: a retrograde double labeling study. J. Comp. Neurol 333, 199–209. [PubMed: 8393892]

Tomassini V, Jbabdi S, Klein JC, Behrens TE, Pozzilli C, Matthews PM, Rushworth MF, Johansen-Berg H, 2007. Diffusion-weighted imaging tractography-based parcellation of the human lateral premotor cortex identifies dorsal and ventral subregions with anatomical and functional specializations. J. Neurosci 27, 10259–10269. [PubMed: 17881532]

Tombari D, Loubinoux I, Pariente J, Gerdelat A, Albucher JF, Tardy J, Cassol E, Chollet F, 2004. A longitudinal fMRI study: in recovering and then in clinically stable sub-cortical stroke patients. Neuroimage 23, 827–839. [PubMed: 15528083]

van Meer MP, van der Marel K, Wang K, Otte WM, El Bouazati S, Roeling TA, Viergever MA, Berkelbach van der Sprenkel JW, Dijkhuizen RM, 2010. Recovery of sensorimotor function after experimental stroke correlates with restoration of resting-state interhemispheric functional connectivity. J. Neurosci 30, 3964–3972. [PubMed: 20237267]

Author Manuscript

Author Manuscript

Author Manuscript

Author Manuscript

Wang L, Yu C, Chen H, Qin W, He Y, Fan F, Zhang Y, Wang M, Li K, Zang Y, Woodward TS, Zhu C, 2010. Dynamic functional reorganization of the motor execution network after stroke. Brain 133, 1224–1238. [PubMed: 20354002]

Ward NS, Brown MM, Thompson AJ, Frackowiak RS, 2003. Neural correlates of motor recovery after stroke: a longitudinal fMRI study. Brain 126, 2476–2496. [PubMed: 12937084]

Weber R, Ramos-Cabrer P, Justicia C, Wiedermann D, Strecker C, Sprenger C, Hoehn M, 2008. Early prediction of functional recovery after experimental stroke: functional magnetic resonance imaging, electrophysiology, and behavioral testing in rats. J. Neurosci 28, 1022–1029. [PubMed: 18234880]

Weiller C, Chollet F, Friston KJ, Wise RJ, Frackowiak RS, 1992. Functional reorganization of the brain in recovery from striatocapsular infarction in man. Ann. Neurol 31, 463–472. [PubMed: 1596081]
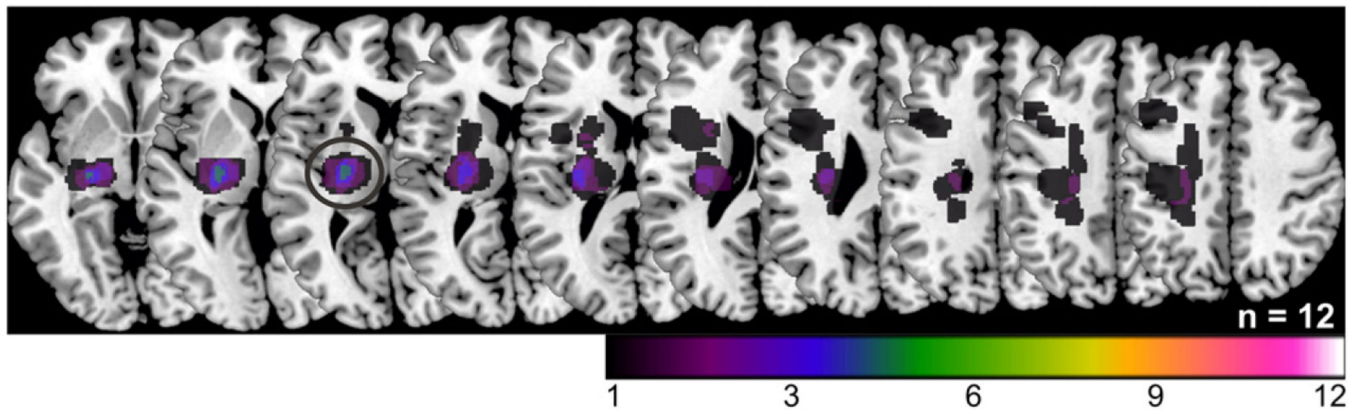
Fig. 1.

DWI lesion maps normalized to MNI space and superimposed on a canonical template as provided by MRIcron. Colour coding indicates lesion overlap. The greatest overlap was at the level of the posterior limb of the internal capsule (black circle).
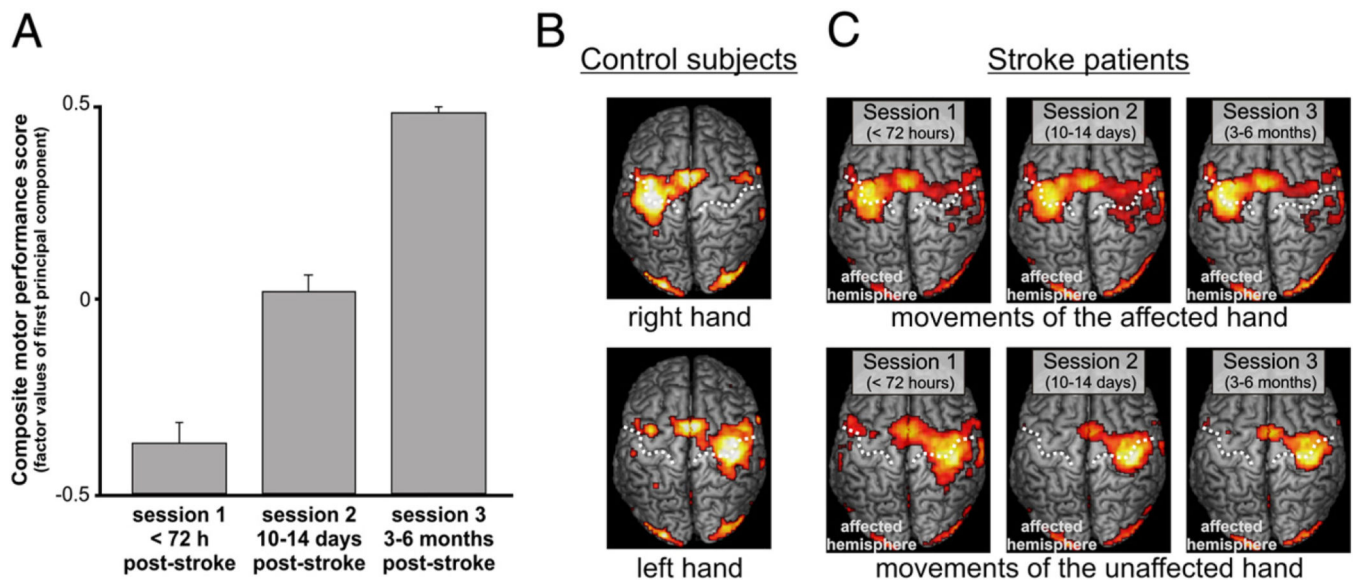
Fig. 2.
(A) Mean composite motor performance scores (and SE) at different sessions post-stroke. The motor scores represent the factor values of the first principal component resulting from a PCA with the ARAT score and the grip force index as input variables. (B) BOLD signal changes in healthy subjects during movements of the left or right hand. (C) BOLD signal changes in patients during movements of the affected or unaffected hand at different stages post-stroke ($p<0.05$ FDR-corrected). The dashed line defines the course of the central sulcus.
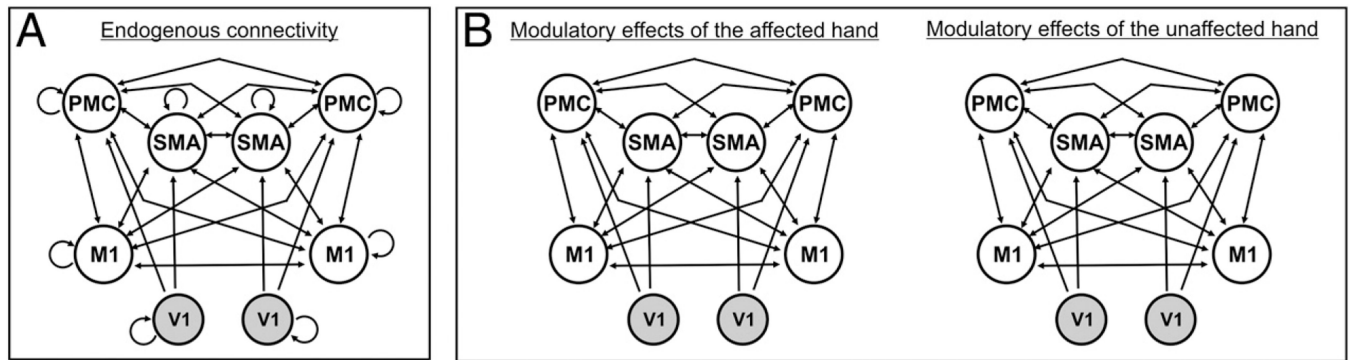
Fig. 3.
Regions of interest and model showing the best model fit according to Bayesian Model Selection (BMS) (Stephan et al., 2009). (A) Connectivity model for endogenous (i.e., task-independent) neural coupling (DCM A-matrix). (B) Task-dependent modulations of connectivity for movements of the right/affected and the left/unaffected hand (DCM B-matrix). Connections between V1 and contralateral premotor areas (PMC, SMA) are not shown. M1, primary motor cortex; PMC, ventral premotor cortex; SMA, supplementary motor area; V1, primary visual cortex.
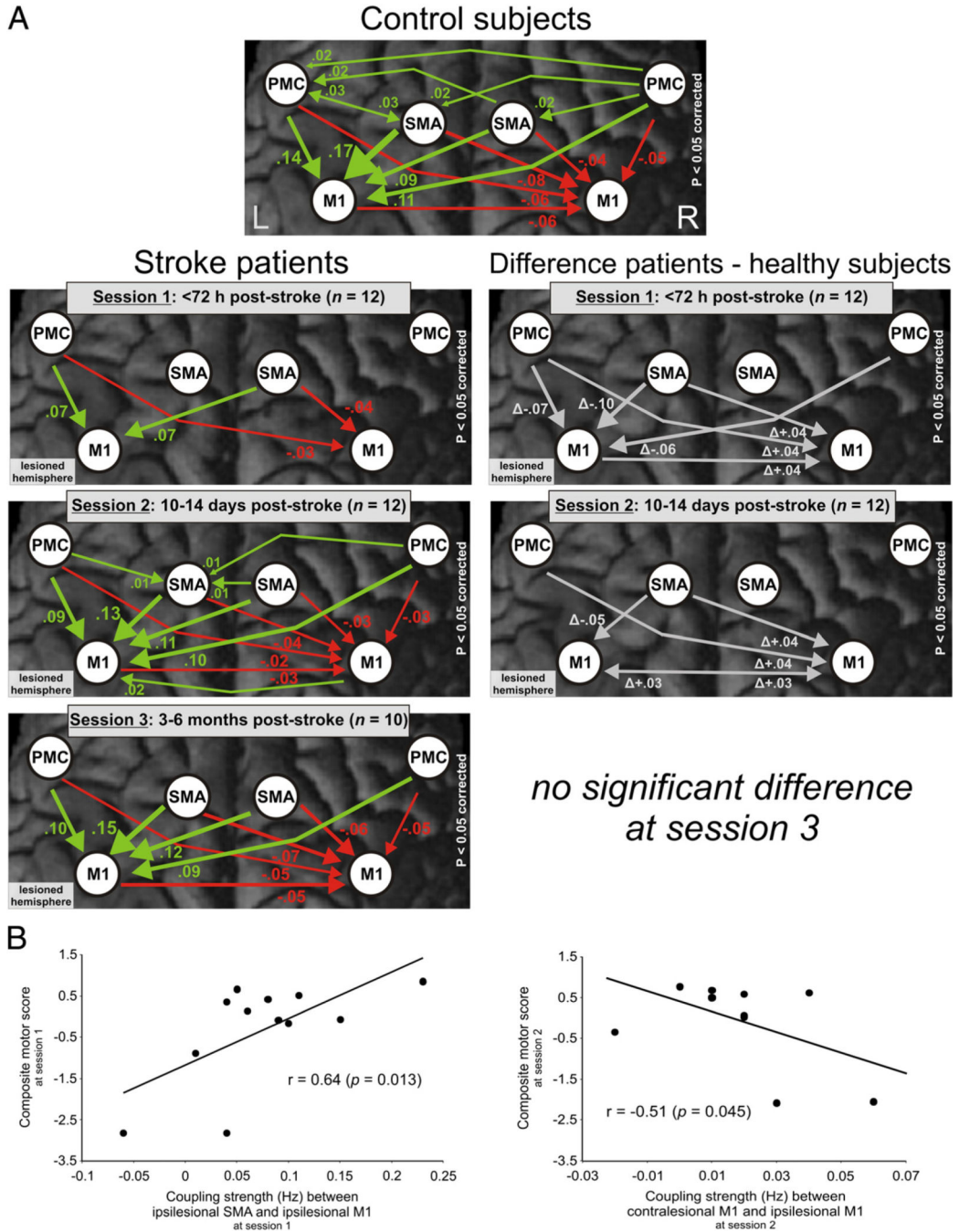
Fig. 4.
(A) Modulation of the cortical motor network during movements of the right hand in healthy subjects and the affected hand in stroke patients at different sessions post-stroke (left column) (p<0.05 FDR-corrected). The right column shows the difference in coupling strength between patients and controls at different sessions (p<0.05 corrected for multiple comparisons; Dunn, 1961). Positive coupling parameters (green arrows) indicate promoting influences, negative coupling parameters (red arrows) indicate inhibitory influences (Friston et al., 2003). Thickness of arrows corresponds to coupling strength. Note that a positive
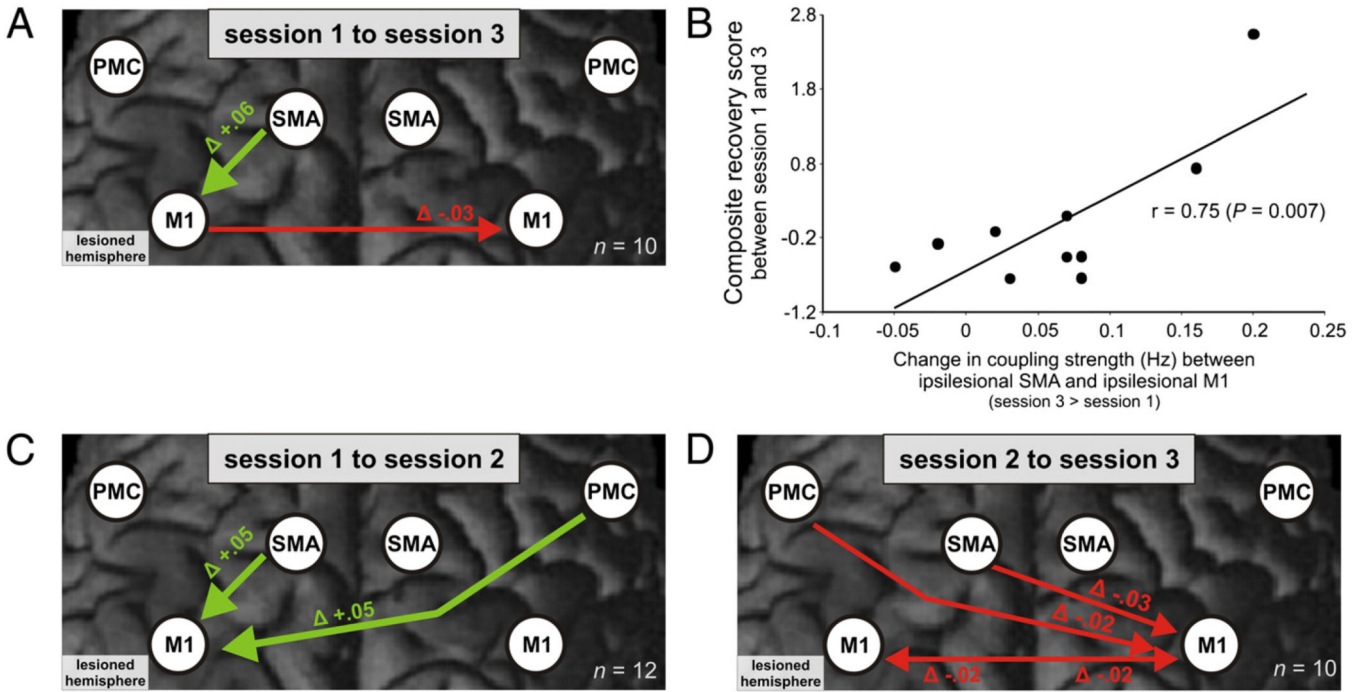
difference in negative (i.e., inhibitory) coupling parameters between patients and control subjects denotes a reduction of inhibitory influences ("disinhibition"). (B) Pearson's correlations between significantly altered coupling parameters as compared to healthy subjects and composite motor scores at session 1 and at session 2.

Fig. 5.
Longitudinal changes in significantly altered coupling parameters as compared to healthy subjects during movements of the affected hand in stroke patients. (A) Changes from session 1 to session 3 (*n*=10). (B) Correlation between increase in ipsilesional SMA–M1 coupling and composite motor recovery scores (i.e., factor values of the first principal component resulting from a PCA of the differences in the ARAT score and the gripforce index between sessions 1 and 3). (C) Changes from session1 to session 2 (*n*=12). (D) Changes from session 2 to session 3 (*n*=10).
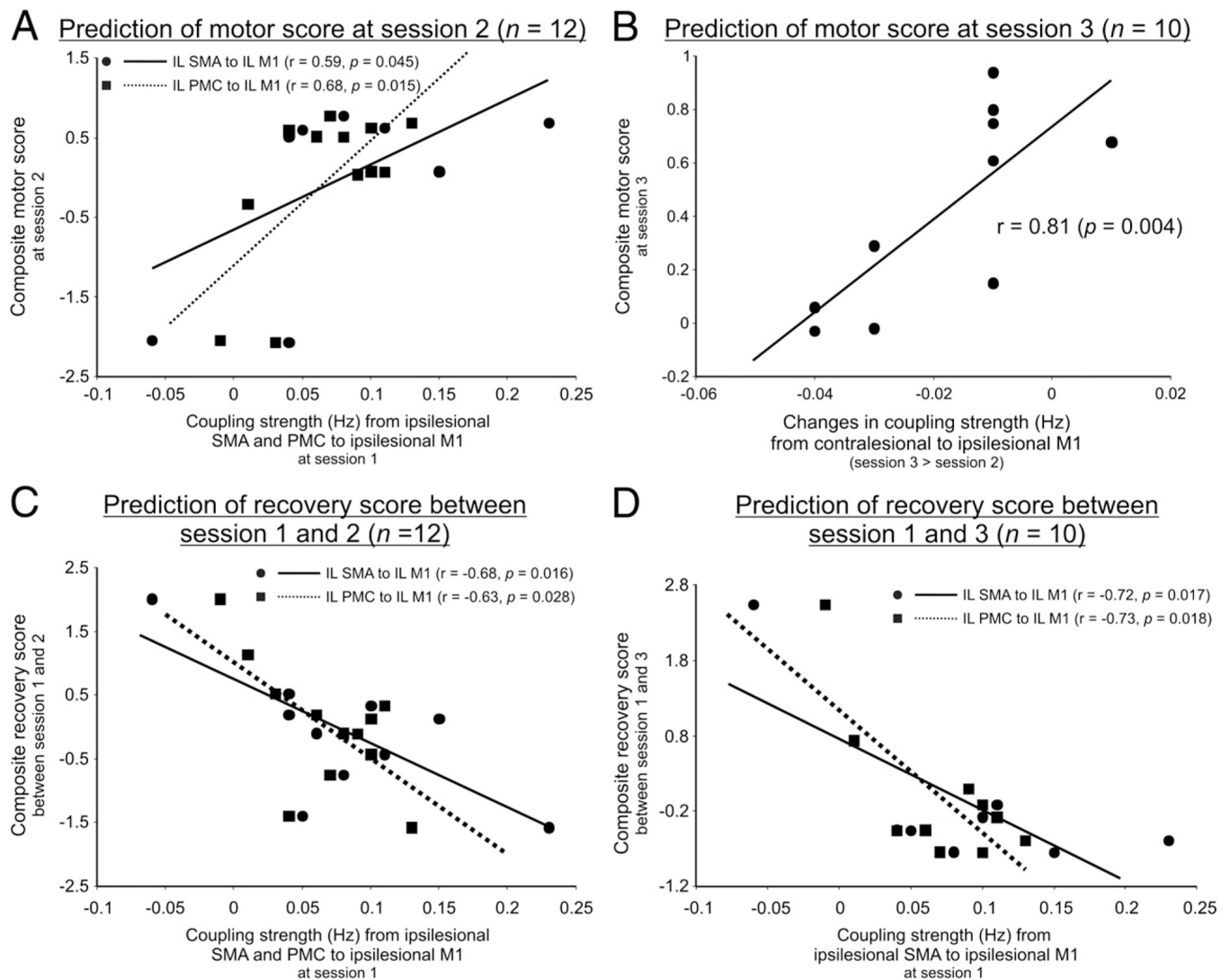
Fig. 6.
Prediction of motor performance and motor recovery after stroke. (A) Correlations between composite motor scores at session 2 and coupling parameters at session 1. (B) Correlation between composite motor scores at session 3 and changes in coupling parameters from sessions 2 to 3. (C) Correlation between motor recovery from sessions 1 to 2 and coupling parameters at session 1. (D) Correlation between motor recovery from sessions 1 to 3 and coupling parameters at session 1.

Author Manuscript Author Manuscript Author Manuscript Author Manuscript

Table 1

Clinical details.

Pat. no.	Gender	Age	Lesion site	Lesion volume (mm³)	ARAT[a] Session 1	ARAT[a] Session 2	ARAT[a] Session 3	Motor score[b] Session 1	Motor score[b] Session 2	Motor score[b] Session 3
1	m	64	R CR	156	50	57	57	−0.11	0.25	0.15
2	f	84	L CR, PG	35168	0	11	53	−2.61	−1.93	0.06
3	m	59	L IC	6575	54	56	57	0.19	0.44	0.29
4	m	53	R PG	9220	54	57	57	0.81	0.83	0.68
5	f	77	R CR, BG, IC	39719	53	53	–	0.35	0.42	–
6	m	61	L IC, thalamus	3737	55	57	57	0.43	0.60	0.80
7	f	69	L IC	10234	38	41	47	0.04	0.23	0.61
8	m	72	L IC	1377	56	57	57	0.96	0.70	0.94
9	m	69	R CR	2880	56	57	57	0.67	0.55	0.75
10	m	68	L IC	2313	43	44	57	0.06	0.28	−0.03
11	f	59	R IC	5282	0	0	–	−2.61	−2.45	–
12	m	64	R PG	10790	28	49	55	−1.16	−0.36	−0.02
Mean (SD)		67 (9)		10621 (13030)	41 (21)	45 (19)	55 (3)			

Session 1 (median: 2 days post-stroke), session 2 (median: 11 days), session 3 (median: 4 months). BG, basal ganglia; CR, corona radiata; IC, internal capsule; L, left; PG, precentral gyrus; R, right.

[a] Action research arm test score for the affected hand (maximum score: 57).

[b] Factor values from the first principal component resulting from a PCA of the ARAT score of the affected hand and the grip force index. Note that negative values do not imply deterioration of motor performance but poorer motor performance compared to the whole group.

Table 2

Mean differences between patients and healthy subjects in effective connectivity among motor areas in the context of affected hand movements (right-hand movements for healthy subjects) (DCM B-matrix) (follow-up tests for significant interaction effects from a 2 (group)×30 (connection) ANOVA corrected for multiple comparisons, Dunn et al., 1961).

Connection modulated by affected/right-hand movements	Mean (SD) coupling strength for controls [a]	Mean (SD) coupling strength for patients [a]	Mean in coupling strength (SEM) (patients−controls)	Correlation with composite motor performance score [b]
Session 1 (72 hours post-stroke, n=12)				
IL PMC–IL M1	+0.1717 (0.0346)	+0.0749 (0.0728) n.s.[c]	−0.097 (0.023)	r=0.64 (p=0.013)
IL PMC–IL M1	+0.1392 (0.0667)	+0.0667 (0.0432)	−0.072 (0.023)	r=0.71 (p=0.005)
CL PMC–IL M1	+0.1075 (0.0443)	+0.0488 (0.0720) n.s.[c]	−0.059 (0.024)	n.s.
IL SMA–CL M1	−0.0783 (0.0565)	−0.0385 (0.0325) n.s.[c]	+0.040[d] (0.019)	n.s.
IL PMC–CL M1	−0.0600 (0.0426)	−0.0258 (0.0135)	+0.034[d] (0.013)	n.s.
IL M1–CL M1	−0.0592 (0.0332)	−0.0176 (0.0243) n.s.[c]	+0.042[d] (0.012)	r=−0.50 (p=0.048)
Session 2 (10–14 days post-stroke, n=12)				
IL SMA–IL M1	+0.1717 (0.0346)	+0.1260 (0.0514)	−0.046 (0.018)	n.s.
CL M1–IL M1	−0.0142 (0.0326) n.s.[c]	0.0187 (0.0199)	+0.033[d] (0.011)	r=−0.51 (p=0.045)
IL SMA–CL M1	−0.0783 (0.0565)	−0.0367 (0.0335)	+0.042[d] (0.019)	n.s.
IL M1–CL M1	−0.0592 (0.0332)	−0.0299 (0.0253)	+0.029[d] (0.012)	n.s.
IL PMC–CL M1	−0.0600 (0.0426)	−0.0237 (0.0215)	+0.036[d] (0.014)	n.s.

CL, contralesional; IL, ipsilesional; M1, primary motor cortex; n.s., not significant, i.e., $p>0.05$ corrected; PMC, ventral premotor cortex; SEM, standard error of the mean; SMA, supplementary motor area.

[a] Positive coupling parameters indicate promoting influences, negative coupling parameters indicate inhibitory influences.

[b] Composite motor scores represent the factor values of the first principal component resulting from a PCA of the ARAT score for the affected hand and the grip force index at the respective session.

[c] Coupling parameter was not different from zero in a one-sample t-test within the respective group ($p<0.05$ FDR-corrected).

[d] Positive differences in inhibitory connections indicate a reduction in inhibition (i.e., "disinhibition").

Table 3

Longitudinal changes in effective connectivity during affected hand movements in stroke patients for coupling parameters showing significant alterations compared to healthy subjects (see Table 2).

Connection modulated by affected hand movements	Mean (SD) coupling strength controls[a]	Mean in coupling (SEM) across time	Correlation with composite motor recovery score[b]
Changes from session 1 to session 3 (n=10)			
IL SMA–IL M1	+0.1717 (0.0346)	+0.064 (0.024)	r=0.75 (p=0.007)
IL M1–CL M1	−0.0592 (0.0332)	−0.030[d] (0.009)	n.s.
Changes from session 2 to session 3 (n=10)			
IL SMA–CL M1	−0.0783 (0.0565)	−0.028[d] (0.008)	n.s.
IL M1–CL M1	−0.0600 (0.0426)	−0.015[d] (0.006)	n.s.
IL PMC–CL M1	−0.0600 (0.0426)	−0.018[d] (0.006)	n.s.
CL M1–IL M1	−0.0142 (0.0326) n.s.[c]	−0.019[d] (0.005)	n.s.
Changes from session 1 to session 2 (n=10)			
CL PMC–IL M1	+0.1075 (0.0443)	+0.055 (0.017)	n.s.
Changes from session 1 to session 2 (n=12)			
IL SMA–IL M1	+0.1717 (0.0346)	+0.051 (0.021)	n.s.
CL PMC–IL M1	+0.1075 (0.0443)	+0.051 (0.015)	n.s.

CL, contralesional; IL, ipsilesional; M1, primary motor cortex; n.s., not significant, i.e., $p > 0.05$ corrected; PMC, ventral premotor cortex; SEM, standard error of the mean; SMA, supplementary motor area.

[a] Coupling parameters in healthy subjects are given as a reference frame: positive coupling parameters describe promoting influences, negative coupling parameters describe inhibitory influences.

[b] Composite motor recovery scores represent the factor values of the first principal component resulting from a PCA of ARAT and grip force improvement scores for the respective time interval.

[c] Coupling parameter was not different from zero in a one-sample t-test within the respective group ($p < 0.05$ FDR-corrected).

[d] Negative changes in inhibitory influences indicate an increase in inhibition (i.e., "re-inhibition").